10CUEE CONFERENCE PROCEEDINGS
10th International Conference on Urban Earthquake Engineering
March 1-2, 2013, Tokyo Institute of Technology, Tokyo, Japan

SEISMIC SAFETY AND UNITED STATES DESIGN PRACTICE FOR STEEL-CONCRETE COMPOSITE FRAME STRUCTURES

Mark D. Denavit[1], Jerome F. Hajjar[2], Tiziano Perea[3], and Roberto T. Leon[4]

1) Design Engineer, Stanley D. Lindsey and Associates, Ltd., Atlanta, Georgia, USA
2) Professor and Chair, Dept. of Civil and Environmental Engineering, Northeastern University, Boston, Massachusetts, USA
3) Professor, Dept. de Materiales, Universidad Autónoma Metropolitana, Azcapotzalco, D. F., Mexico
4) David H. Burrows Professor of Construction Engineering, The Charles E. Via, Jr. Department of Civil and Environmental Engineering, Virginia Polytechnic Institute and State University, Blacksburg, Virginia, USA
mdenavit@sdlal.com, jf.hajjar@neu.edu, tperea@correo.azc.uam.mx, rleon@vt.edu

Abstract: In United States design practice, three system performance factors (R, C_d, and Ω_o) characterize the inelastic behavior of structures and are a crucial component of common elastic design methodologies. However, for steel-concrete composite frame systems these factors have been selected based on comparisons to more traditional and well-studied reinforced concrete and structural steel frame systems, without significant quantitative justification. In this study, the seismic behavior of steel-concrete composite moment and braced frames is investigated and rational system performance factors are developed. A set of archetype frames, selected to be representative of the range of frames seen in practice, were designed according to current design specifications. Using a suite of new finite element formulations for composite systems, nonlinear static pushover and transient dynamic analyses were performed on the frames. The results of the analyses served as statistical data on the seismic response from which the performance factors were quantified. The results from this investigation enable a better understanding of the variability in collapse performance of composite frame systems and will facilitate more effective designs of these systems.

1. INTRODUCTION

A key component of seismic design in the United States is the allowance for inelasticity in structural elements subjected to severe earthquake ground motions. However, static elastic analysis is prevalent for seismic design in current practice. Because of this, seismic performance factors have been developed. The factors are: the response modification factor, R, used in reducing seismic forces determined through elastic methods; the displacement amplification factor, C_d, used in amplifying displacements determined through elastic methods; and the system overstrength factor, Ω_o, used to estimate the actual strength as compared the to the design strength.

These three factors are tabulated for a variety of seismic force resisting systems in national codes (ASCE 2010), however, they have been somewhat arbitrarily assigned. Many R factors were based largely on judgment and qualitative comparisons to the relatively few seismic force resisting systems that had known response capabilities (FEMA 2009). This is particularly true for composite moment and braced frames where the seismic performance factors were assigned based on comparisons to similar structural steel and reinforced concrete systems.

A methodology has been developed to provide a rational basis for determining seismic performance factors which provide equivalent safety against collapse for buildings with different seismic force resisting systems (FEMA 2009). Equivalent safety is provided through an acceptably low probability of structural collapse common to all systems. Structural collapse in the methodology is defined in the context of incremental dynamic analysis, in which nonlinear time history analyses are performed at increasing magnitudes of seismic loading until the structure achieves its peak strength or predefined displacement limits. In this approach, no explicit modeling of collapse is included. Statistical data is generated from the analyses for a set of archetype models and uncertainty is approximated based on the level of knowledge of the particular system and accuracy of the analysis.

This paper presents a study to investigate the behavior of composite frames under seismic loading and to develop rational seismic performance factors following the methodology given in FEMA P-695 Quantification of Building Seismic Performance Factors (FEMA 2009).

2. SEISMIC FORCE RESISTING SYSTEMS

Two separate seismic force resisting systems are analyzed in this study: composite special moment frames (C-SMF) and composite special concentrically braced frames (C-SCBF). The current seismic performance factors for these two systems are given in Table 1 (ASCE 2010).

Table 1. Current Seismic Performance Factors

System	Ω_o	R	C_d
C-SMF	3.0	8.0	5.5
C-SCBF	2.0	5.0	4.5

The requirements for composite special moment frames are described in the AISC *Seismic Specification* (AISC 2010). C-SMFs utilize fully restrained connections and consist of either composite or reinforced concrete columns and either structural steel, concrete-encased composite, or composite beams. They are expected to provide significant inelastic deformation capacity through flexural yielding of the beams and limited yielding of the column panel zones. Columns are designed to be stronger than the fully yielded and strain-hardened beams, although flexural yielding in columns at the base is permitted.

The requirements for composite special concentrically braced frames are described in the AISC *Seismic Specification* (AISC 2010). C-SCBFs consist of CFT or SRC composite columns, structural steel or composite beams, and structural steel or CFT braces. They are expected to provide significant inelastic deformation capacity primarily through brace buckling and yielding of the brace in tension.

3. ARCHETYPE FRAMES

To perform the methodology, it is necessary to have a suite of frames (termed index archetypes) for which the analyses can be performed. Ideally that suite of frames is representative of the entire range of frames seen in practice. However, it is generally recognized within the methodology that a practical number of frames cannot fully represent the permissible range, thus simplifications must be made. The selected frames are described below; complete details including the design process are presented in Denavit (2012).

The building layout is the same for each of the index archetype configurations: 3 bays by 5 bays with a bay width of either 20 ft or 30 ft (Figure 1). The buildings are 3 or 9 stories tall with a story height of 13 ft. For the moment frames the columns were either RCFTs or SRCs. For the braced frames the columns were CCFTs and the braces were either rectangular HSS or wide flange in a two-story X configuration. A composite floor system was assumed for all configurations, although the beams in the seismic force resisting systems were designed and analyzed assuming bare steel.

Two levels of gravity load were selected: "high" which corresponded to warehouse live loading (250 psf) and the interior frame and "low" which corresponded to office live loading (65 psf) and the exterior frame. Two levels of seismic load were selected corresponding to the levels design earthquake associated with the maximum (D_{max}) and minimum (D_{min}) of seismic design category D (ASCE 2010).

The methodology prescribes that $C_d = R$ (FEMA 2009), which is contrary to current practice (ASCE 2010) where C_d is typically less than R (Table 1). For deformation-controlled structures, such as moment frames, this change results in larger member sizes. In this study, most frames were designed assuming $C_d = R$, however, a subset of the moment frames were duplicated and designed with the current value (C_d = 5.5) so as to compare to the current state of design practice.

In total, 60 frames were selected and designed for this study. The frames varied in building height, column type, concrete strength, level of seismic load, level of gravity load, and bay width. Details of the frames are given in Table 2 for the C-SMFs and Table 3 for the C-SCBFs.

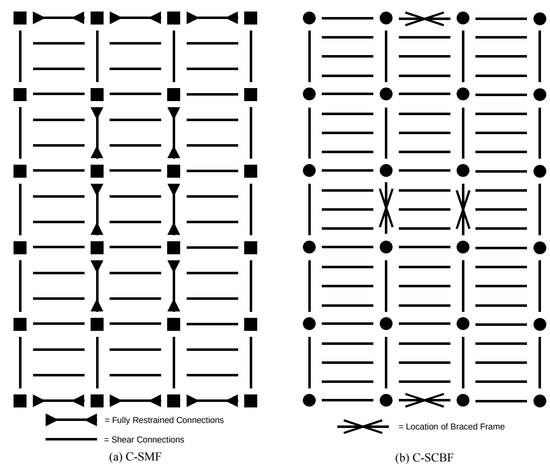

Figure 1. Building Layout

3.1 Material Strengths

Two sets of material strengths are used in this study as summarized in Table 4. The first is the nominal strength which is used in the design of the archetypes. The second is the expected strengths which are used in the analyses of the archetypes. The nominal strengths are selected as typical material properties. The expected strengths for the steel materials are defined as described in Section A3.2 of the AISC *Seismic Specification* (AISC 2010). For lack of a more appropriate definition, the expected strengths for the concrete materials are defined as the required average compressive strength from field strength tests when data are not available to establish a sample standard deviation as described in Section 5.3.2.2 of the ACI *Code* (ACI 2011).

3.2 Seismic Design

The equivalent lateral force method (ASCE 2010) was used for the seismic design. The level of seismic loading is defined in terms of the seismic design category. The frames in this study were designed for seismic design category D at either the maximum (D_{max}) or minimum (D_{min}).

Table 2. Frame Information: C-SMFs

Frame #	Name	Number of Stories	Gravity Load	f'$_c$	Bay Width	SDC	C_d = R	T	V	Building W	C_s	Frame V
				ksi	*ft*			*s*	*kips*	*kips*		*kips*
1	RCFT-3-1	3	high	4	20	Dmax	yes	0.437	307.8	2,462	0.125	153.9
2	RCFT-3-2	3	high	12	20	Dmax	yes	0.437	307.8	2,462	0.125	153.9
3	RCFT-3-3	3	high	4	20	Dmin	yes	0.468	131.5	2,462	0.053	65.7
4	RCFT-3-4	3	high	12	20	Dmin	yes	0.468	131.5	2,462	0.053	65.7
5	RCFT-3-5	3	high	4	30	Dmax	yes	0.437	670.3	5,363	0.125	335.2
6	RCFT-3-6	3	high	12	30	Dmax	yes	0.437	670.3	5,363	0.125	335.2
7	RCFT-3-7	3	high	4	30	Dmin	yes	0.468	286.3	5,363	0.053	143.2
8	RCFT-3-8	3	high	12	30	Dmin	yes	0.468	286.3	5,363	0.053	143.2
9	RCFT-3-9	3	low	4	20	Dmax	yes	0.437	229.0	1,832	0.125	114.5
10	RCFT-3-10	3	low	12	20	Dmax	yes	0.437	229.0	1,832	0.125	114.5
11	RCFT-3-11	3	low	4	20	Dmin	yes	0.468	97.8	1,832	0.053	48.9
12	RCFT-3-12	3	low	12	20	Dmin	yes	0.468	97.8	1,832	0.053	48.9
13	RCFT-3-13	3	low	4	30	Dmax	yes	0.437	493.1	3,945	0.125	246.6
14	RCFT-3-14	3	low	12	30	Dmax	yes	0.437	493.1	3,945	0.125	246.6
15	RCFT-3-15	3	low	4	30	Dmin	yes	0.468	210.7	3,945	0.053	105.3
16	RCFT-3-16	3	low	12	30	Dmin	yes	0.468	210.7	3,945	0.053	105.3
17	RCFT-9-1	9	high	4	20	Dmax	yes	0.996	618.6	8,216	0.075	309.3
18	RCFT-9-3	9	high	4	20	Dmin	yes	1.067	192.5	8,216	0.023	96.2
19	RCFT-9-5	9	high	4	30	Dmax	yes	0.996	1,343.3	17,841	0.075	671.7
20	RCFT-9-7	9	high	4	30	Dmin	yes	1.067	417.9	17,841	0.023	209.0
21	RCFT-9-9	9	low	4	20	Dmax	yes	0.996	428.9	5,696	0.075	214.4
22	RCFT-9-11	9	low	4	20	Dmin	yes	1.067	133.4	5,696	0.023	66.7
23	RCFT-9-13	9	low	4	30	Dmax	yes	0.996	916.4	12,171	0.075	458.2
24	RCFT-9-15	9	low	4	30	Dmin	yes	1.067	285.1	12,171	0.023	142.6
25	SRC-3-1	3	high	4	20	Dmax	yes	0.437	307.8	2,462	0.125	153.9
26	SRC-3-2	3	high	12	20	Dmax	yes	0.437	307.8	2,462	0.125	153.9
27	SRC-3-3	3	high	4	20	Dmin	yes	0.468	131.5	2,462	0.053	65.7
28	SRC-3-4	3	high	12	20	Dmin	yes	0.468	131.5	2,462	0.053	65.7
29	SRC-3-9	3	low	4	20	Dmax	yes	0.437	229.0	1,832	0.125	114.5
30	SRC-3-10	3	low	12	20	Dmax	yes	0.437	229.0	1,832	0.125	114.5
31	SRC-3-11	3	low	4	20	Dmin	yes	0.468	97.8	1,832	0.053	48.9
32	SRC-3-12	3	low	12	20	Dmin	yes	0.468	97.8	1,832	0.053	48.9
33	RCFT-3-1-Cd	3	high	4	20	Dmax	no	0.437	307.8	2,462	0.125	153.9
34	RCFT-3-3-Cd	3	high	4	20	Dmin	no	0.468	131.5	2,462	0.053	65.7
35	RCFT-3-9-Cd	3	low	4	20	Dmax	no	0.437	229.0	1,832	0.125	114.5
36	RCFT-3-11-Cd	3	low	4	20	Dmin	no	0.468	97.8	1,832	0.053	48.9

Table 3. Frame Information: C-SCBFs

Frame #	Name	Number of Stories	Gravity Load	f'$_c$	Bay Width	SDC	C_d = R	T	V	Building W	C_s	Frame V
				ksi	*ft*			*s*	*kips*	*kips*		*kips*
1	CCFT-3-1	3	high	4	20	Dmax	yes	0.437	492.4	2,462	0.200	246.2
2	CCFT-3-2	3	high	12	20	Dmax	yes	0.437	492.4	2,462	0.200	246.2
3	CCFT-3-3	3	high	4	20	Dmin	yes	0.468	210.3	2,462	0.085	105.2
4	CCFT-3-4	3	high	12	20	Dmin	yes	0.468	210.3	2,462	0.085	105.2
5	CCFT-3-5	3	high	4	30	Dmax	yes	0.437	1,072.5	5,363	0.200	536.3
6	CCFT-3-6	3	high	12	30	Dmax	yes	0.437	1,072.5	5,363	0.200	536.3
7	CCFT-3-7	3	high	4	30	Dmin	yes	0.468	458.2	5,363	0.085	229.1
8	CCFT-3-8	3	high	12	30	Dmin	yes	0.468	458.2	5,363	0.085	229.1
9	CCFT-3-9	3	low	4	20	Dmax	yes	0.437	366.4	1,832	0.200	183.2
10	CCFT-3-10	3	low	12	20	Dmax	yes	0.437	366.4	1,832	0.200	183.2
11	CCFT-3-11	3	low	4	20	Dmin	yes	0.468	156.5	1,832	0.085	78.3
12	CCFT-3-12	3	low	12	20	Dmin	yes	0.468	156.5	1,832	0.085	78.3
13	CCFT-3-13	3	low	4	30	Dmax	yes	0.437	789.0	3,945	0.200	394.5
14	CCFT-3-14	3	low	12	30	Dmax	yes	0.437	789.0	3,945	0.200	394.5
15	CCFT-3-15	3	low	4	30	Dmin	yes	0.468	337.0	3,945	0.085	168.5
16	CCFT-3-16	3	low	12	30	Dmin	yes	0.468	337.0	3,945	0.085	168.5
17	CCFT-9-1	9	high	4	20	Dmax	yes	0.996	989.8	8,216	0.120	494.9
18	CCFT-9-3	9	high	4	20	Dmin	yes	1.067	307.9	8,216	0.037	154.0
19	CCFT-9-5	9	high	4	30	Dmax	yes	0.996	2,149.3	17,841	0.120	1074.7
20	CCFT-9-7	9	high	4	30	Dmin	yes	1.067	668.7	17,841	0.037	334.3
21	CCFT-9-9	9	low	4	20	Dmax	yes	0.996	686.2	5,696	0.120	343.1
22	CCFT-9-11	9	low	4	20	Dmin	yes	1.067	213.5	5,696	0.037	106.7
23	CCFT-9-13	9	low	4	30	Dmax	yes	0.996	1,466.3	12,171	0.120	733.1
24	CCFT-9-15	9	low	4	30	Dmin	yes	1.067	456.2	12,171	0.037	228.1

The seismic base shear, V, is defined as the product of the effective seismic weight, W, and the seismic coefficient, C_s, determined based on the fundamental period, T, in accordance with Section 12.8 of ASCE 7 (ASCE 2010). The effective seismic weight of the building is determined in accordance with Section 12.7.2 of ASCE 7 (ASCE 2010).

The effective seismic weight, W, is the sum of the following:

- 100% of the dead load
- 25% of the warehouse floor live load (which is deemed storage)
- 15.4% of the office floor live load (equivalent to 10 psf for partitions)

Table 4. Nominal and Expected Material Strengths

Material	Nominal Strength (Used for Design)	Expected Strength (Used for Analysis)
Circular HSS (ASTM A500 Gr. B)	F_y = 42 ksi F_u = 58 ksi	F_y = 58.8 ksi F_u = 75.4 ksi
Rectangular HSS (ASTM A500 Gr. B)	F_y = 46 ksi F_u = 58 ksi	F_y = 64.4 ksi F_u = 75.4 ksi
Wide Flange (ASTM A992)	F_y = 50 ksi F_u = 65 ksi	F_y = 55.0 ksi F_u = 71.5 ksi
Reinforcement (ASTM A615)	F_{yr} = 60 ksi F_u = 90 ksi	F_{yr} = 75.0 ksi F_u = 112.5 ksi
Plate (ASTM A572 Gr. 50)	F_y = 50 ksi F_u = 65 ksi	F_y = 55.0 ksi F_u = 78.0 ksi
4 ksi Concrete	f'_c = 4 ksi	f'_c = 5.2 ksi
12 ksi Concrete	f'_c = 12 ksi	f'_c = 13.9 ksi

4. NONLINEAR ANALYSIS MODEL

The nonlinear analysis models consist of beam and zero length elements representing the seismic force resisting frame and nonlinear truss elements representing the destabilizing effect of the remainder of the building that is tributary to the frame. Key details of the model are presented here; full details are presented elsewhere (Denavit 2012).

The beam element used in the model is a distributed plasticity formulation developed specifically for steel-concrete composite frames. The element uses a mixed basis (i.e., using both displacements and forces as primary variables) to allow for accurate modeling of both material and geometric nonlinearities. Fiber sections and uniaxial cyclic constitutive relations are used to model cross section behavior. The concrete and steel material models account for the salient features of each material, as well as the interaction between the two, including concrete confinement and local buckling.

The connection region of special moment frames is modeled as shown in Figure 2. Key components are a rigid link parallelogram model with a rotational spring representing the nonlinear panel zone behavior and elastic beam elements which serve to move the beam plastic hinges to specified locations. Nonlinear beam elements for the columns and beams frame into this connection model. The connecting elements (e.g., split tees as shown in Figure 2) are not explicitly modeled since they are designed to not experience significant deformations, even under large frame deformations.

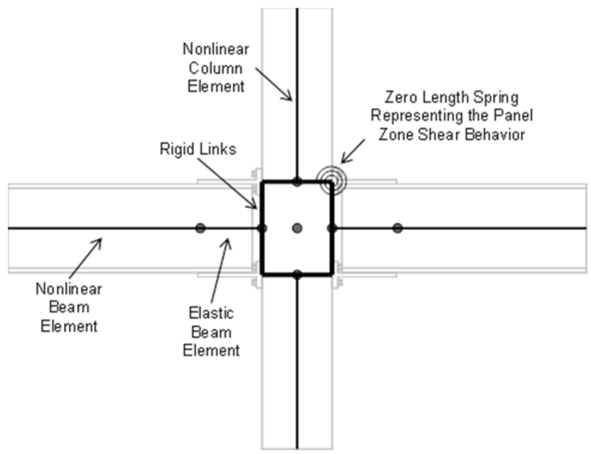

Figure 2. Schematic of the Connection Region of Special Moment Frames

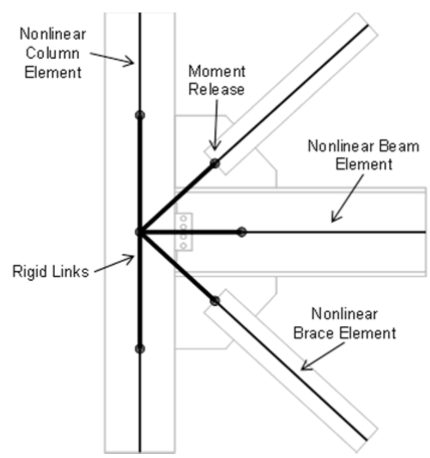

Figure 3. Schematic of the Beam-To-Column Connection Region of Special Concentrically Braced Frames

Connection regions in special concentrically braced frames have large gusset plates that serve to stiffen the connections. Hsiao et al. (2012) developed recommendations for modeling the connection region of steel special concentrically braced frames. A simplified version of the model by Hsiao et al. (2012) is used in this work. The beam-to-column connection region is modeled as shown in Figure 3. Rigid links are used to model the region where the gusset plate stiffens the beam, brace, and column. The length of the rigid link along the column is equal to the distance from the work point to the top of the gusset plate. The length of the rigid link along the brace is equal to the distance from the work point to the physical brace. The length of the rigid link along the beam is equal to the distance from the work point to column face plus 75% of the distance from the column face to the edge of the gusset plate. The column and beam frame directly into the rigid link whereas a moment release is used between the rigid link and the brace.

The analyses were performed in two-dimensions. The mesh density was selected such that the model was refined enough to obtain accurate results, but not so dense as to introduce the ill-effects of localization. The nominal length of the column elements was one-third of the story height. The nominal length of the girder elements was one-third of the bay width for the C-SMFs and one-fourth of the bay width for the C-SCBFs corresponding to the beam spacing (Figure 1). Three integration points were used for all beam elements. Nominal size of the strips in the fiber discretization was 1/20th of the section depth, with the number of fibers in each component defined based on this fixed ratio and rounded up to the nearest integer.

The braces in the C-SCBFs are assumed to be physically oriented such that weak axis buckling is out-of-plane of the frame. However, in the model the brace is oriented such that weak axis buckling is in-plane to allow for the use of a two-dimensional model. Correspondingly, the moment releases at the brace ends represent the relatively weak out-of-plane rotational strength of the gusset plate.

As prescribed in the methodology (FEMA 2009), prior to application of the lateral load (either static or dynamic), gravity load equal to 105% of the dead load plus 25% of the live load and roof live load was applied and held constant for the remainder of the analysis. All gravity loads were applied as nodal loads based on tributary areas.

The methodology (FEMA 2009) does not explicitly define the mass to be used in the analyses. Thus, mass was assigned to the structure based on the effective seismic weight computed for design. For nodes with gravity load, the two translational DOFs were assigned equal masses equivalent to the dead load plus a percentage of the live load. Additionally, for numerical stability, a minimum nominal mass was assigned to all degrees-of-freedom. The value of the minimum nominal mass was 1×10^{-6} kip-s^2/in for the translational DOFs and 1×10^{-6} kip-in-s^2 for the rotational DOFs. Also for numerical stability, an additional elastic stiffness of EA = 300 and EI = 3000 was added to each brace section (e.g., in the event of significant yielding along the full length of the member). Rayleigh damping was used, defined as 2.5% in the 1st and 3rd modes based on recommendations from the methodology (FEMA 2009).

A summary of the gravity load cases and mass used in both the design and the analysis of the archetype frames is presented in Table 5.

The model accurately captures member plasticity, local buckling, global buckling, and panel zone behavior as demonstrated through validation studies presented elsewhere (Denavit 2012). However, some aspects of behavior and failure modes have not been modeled.

- Fracture is not included in the model. While fracture is expected during structural collapse, this study is not explicitly modeling collapse. Fracture is not anticipated o control the behavior of well-designed C-SMF, where ductile yielding of the beams in flexure is expected to dominate the response, or C-SCBF, where ductile yielding of the braces and buckling of the braces is expected to dominate the response.
- Connection regions are modeled, however, failure or degradation of the connecting elements is not included in these models. Experimental testing has shown that with proper design and detailing the connecting elements inelasticity can be confined to the member.
- In the design of the frames it was assumed that the beams were provided with lateral bracing sufficient to ensure the full plastic moment capacity could be achieved. Correspondingly, lateral torsional buckling was not included in the model

Table 5. Gravity Load and Mass in Design and Analysis

	Design	Analysis
Gravity Load	$1.4\,D$ $1.2\,D + 1.6\,L + 0.5L_r$ $1.2\,D + 0.5\,L + 1.6L_r$ etc., including live load reduction Section 2.3 (ASCE 2010)	$1.05\,D + 0.25\,L + 0.25\,L_r$ (FEMA 2009)
Mass	D + 25% storage live load + 10 psf for partitions Section 12.7.2 (ASCE 2010)	Same as for design

5. STATIC PUSHOVER ANALYSES

Static pushover analyses were performed on each frame. Lateral loads were applied at each story in fixed ratios based on the story mass and the mode shape of the structure (FEMA 2009). Thus, an eigenvalue analysis was performed prior to the application of lateral load (but after gravity load was applied). The loading was conducted in displacement control until at least a 20% drop in strength after the peak (V_{80}) was observed. Key results from these analyses include:

- The fundamental period from the model, T_1
- The maximum base shear capacity, V_{max}
- The overstrength factor, $\Omega = V_{max}/V$
- The ultimate roof displacement (i.e., at V_{80}), δ_u
- The effective yield roof drift displacement, $\delta_{y,\text{eff}}$, [Equation 1 (FEMA 2009)]
- The period-based ductility, $\mu_T = \delta_u / \delta_{u,\text{eff}}$

$$\delta_{y,eff} = C_o \frac{V_{max}}{W}\left(\frac{g}{4\pi^2}\right)\left(\max(T,T_1)\right)^2 \qquad (1)$$

where,

C_o = A coefficient based on the fundamental mode shape (FEMA 2009)

5.1 Analysis Results

An example of the results for a three-story C-SMF (RCFT columns, high gravity load, f'_c = 4 ksi, SDC = D_{max}) is shown in Figure 4. Full results are presented elsewhere (Denavit 2012).

For the C-SMFs, an initially linear response is observed followed by gradual stiffness reduction up to the peak lateral capacity of the frame then near linear post peak degradation until the analysis was stopped after at least a 20% drop in capacity was observed. For the 3 story frames an even distribution of deformation is seen among the stories with the exception of the roof story of some frames where lower deformations were observed at the V_{80} level. For the 9 story frames, the distribution of deformation was even among the stories at the design base shear level, however, at the maximum base shear and after a 20% drop in capacity, the deformation was concentrated in ranges of 4 to 6 stories forming a multi-story mechanism (Krishnan and Muto 2012). The story groups where the inelasticity was concentrated were either located at the top, middle, or bottom of the structure. No fundamental behavioral differences were observed between the frames with RCFT columns and those with SRC columns owing to the fact that flexural yielding of the beams controlled the response.

For the C-SCBFs, the response was initially linear, however, in contrast to the C-SMFs, sharp changes in stiffness including drops in capacity were observed in the response corresponding to yielding and buckling of the individual braces. These jumps are exacerbated by the fact that only one bay of bracing was modeled; had multiple bays been included with slightly different loading or material properties, the response would likely have been smoother. Also in contrast to the C-SMFs, for the 3 story frames the deformation was often concentrated into one story. The 9 story frames showed a similar response to the C-SMFs in that multi-story mechanisms were developed where the deformation was concentrated in 4 to 6 consecutive stories.

Conclusions from the results are given in Section 7.1 in the context of evaluating the system overstrength factor.

6. DYNAMIC RESPONSE HISTORY ANALYSES

In the methodology, collapse is assessed in the context of incremental dynamic analyses (IDA) (Vamvatsikos and Cornell 2002). Dynamic response history analyses are performed, subjecting each frame to a suite of ground motions scaled at different intensities. The 44 earthquake ground motions described in the methodology (FEMA 2009) were used for this study.

Explicit modeling of the collapse of structures is a challenging task and the subject of current research (Bažant and Verdure 2007; Khandelwal et al. 2009; McAllister et al. 2012; Szyniszewski and Krauthammer 2012). The FEMA (2009) methodology has avoided the need to explicitly model collapse by defining collapse in the context of incremental dynamic analyses. In incremental dynamic analyses, a frame is analyzed under different ground motions and at different intensities. The resulting curve shows a response value (typically peak story drift) versus an intensity measure. Typical results would show an initially high slope, gradually transitioning to a low slope; however, in practice a wide variety of behavior is seen.

Determination of "collapse" is necessary for the methodology and thus approximate definitions are adopted. In this work, collapse is defined when a prescribed maximum story drift of 10% is observed in the incremental dynamic analysis results. This is an approximate method since collapse is not associated with any particular drift limit (Krawinkler et al. 2003); however, some justification of the 10% limit exists. Generally, little hardening response is seen incremental dynamic analysis results beyond 10% drift. Also, the nonlinear models were not validated for deformations beyond this range and nonlinear effects that are not being modeled directly in this work, such as fracture, lateral torsional buckling, or connection degradation may

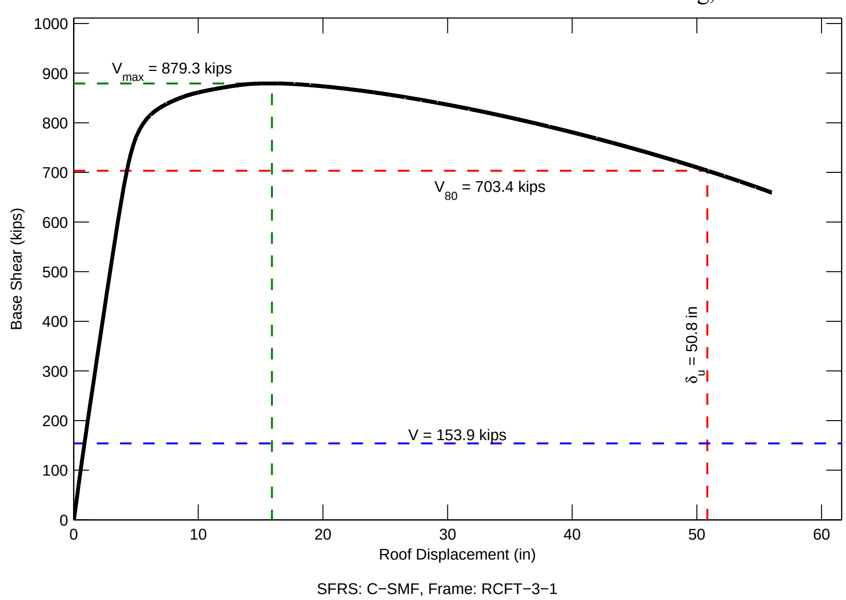

Figure 4. Sample Results of the Static Pushover Analyses

occur at these higher drift levels.

Key results from the dynamic response history analyses include:

- The median collapse intensity, $\hat{S}_{CT}$, determined as the intensity, ST, at which half of the ground motions cause maximum story drifts of greater than 5%
- The collapse margin ratio, CMR = $\hat{S}_{CT}/S_{MT}$ (where S_{MT} is the maximum considered earthquake intensity).

6.1 Analysis Results

An example of the results for the same three-story C-SMF highlighted before is shown in Figure 5. Full results are presented elsewhere (Denavit 2012).

For both the C-SMFs and C-SCBFs, the majority of incremental dynamic analysis curves exhibit the typical response with an initial relatively high slope followed by a relatively low slope at higher intensities. The initial slope of the curves for each frame varies, owing to inherent differences between the 44 ground motions. In general, at the maximum considered earthquake intensity (i.e., $S_T = S_{MT}$), the distribution of story drifts is relatively uniform along the height of the building. An exception is the 9 story C-SCBFs where often the top story exhibits deformations several times greater than that of the other stories.

7. EVALUATION OF SEISMIC PERFORMANCE FACTORS

For the purposes of evaluation, the methodology requires the archetype frames be categorized into performance groups based on the design gravity load level (high or low), design seismic load level (D_{max} or D_{min}), and fundamental period (long or short). Eight performance groups are defined for seismic force resisting system and are used as described below to evaluate each of the seismic performance factors.

7.1 System Overstrength Factor, Ω_o

According to the methodology, the system overstrength factor, Ω_o, should not be taken as less than the largest average value of overstrength, Ω, from any performance group, however, upper limits of 1.5R and 3.0 are applied (FEMA 2009).

For the C-SMFs, the average overstrength for the performance groups ranges from 5.3 (for the performance group with high gravity load, SDC = D_{max}, and long period) to 9.9 (for the performance group with high gravity load, SDC = D_{min}, and long period). These values are quite high and reflect the displacement controlled design of these structures. Other studies on steel special moment frames (NIST 2010) have also shown high overstrength. Several factors have led to the particularly high overstrength values seen in this study. The use of $C_d = R$ in the design of the frames reduced the allowable story drifts thus increasing member sizes. In the model, the plastic hinges were forced to a location 2d/3 away from the column face (where d is the bean section depth). This distance was the assumed length of the connection. Selection of this distance resulted in higher frame strengths as compared to shorter connections. Additionally, reduced beam section connections were not used for these structures; if they had been used, lower overstrength would have been observed. For the results shown, all of the performance groups exceed the practical upper limit of 3.0, so it is recommended that the system overstrength factor remain unchanged from its current value (Ω_o = 3.0).

For the C-SCBFs, the average overstrength for the performance groups ranges from 1.7 (for the performance group with high gravity load, SDC = D_{min}, and short period) to 2.8 (for the performance group with low gravity load, SDC = D_{max}, and short period). These results are in contrast to the C-SMFs where high overstrength was observed and

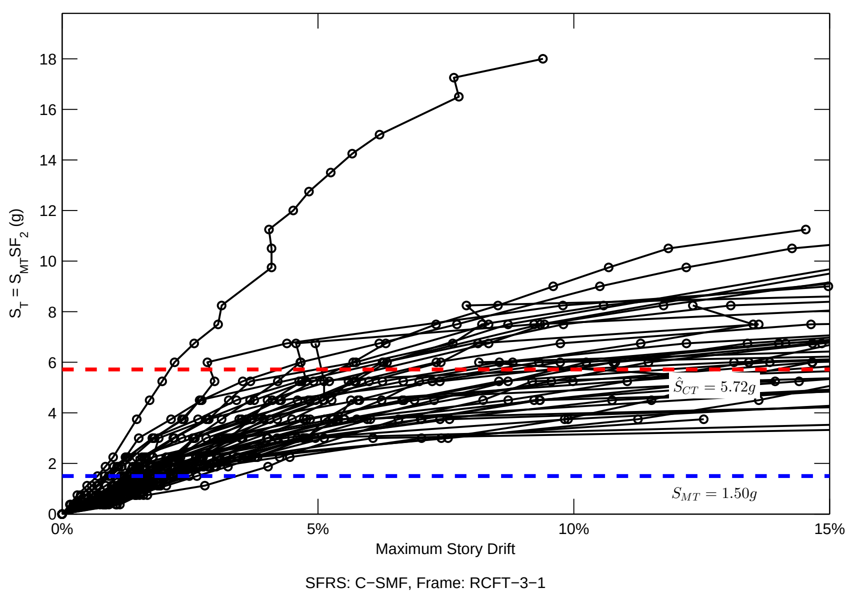

Figure 5. Sample Results of the Dynamic Response History Analyses

reflect the strength controlled design of these structures. Other studies on steel special concentrically frames (NIST 2010) have shown similar overstrength results. In light of these results (some performance groups with overstrength greater than 2.0), an increase the system overstrength factor for C-SCBFs could be warranted, although the current value ($\Omega_o = 2.0$) is likely sufficient.

7.2 Response Modification Factor, *R*

According to the methodology, the response modification factor that was used to design the archetype frames is acceptable if the probability of collapse for maximum considered earthquake ground motions is approximately 20% or less for each index archetype and 10% or less on average for each performance group (FEMA 2009). To evaluate these conditions, adjusted collapse margin ratios are computed and compared against reference values (Equations 2 and 3).

$$ACMR_i \geq ACMR_{20\%} \tag{2}$$

$$\text{mean}\left(ACMR_i\right) \geq ACMR_{10\%} \tag{3}$$

where,

$ACMR_i$ = adjusted collapse margin ratio for each index archetype, *i*

$ACMR_{20\%}$ = acceptable value of the adjusted collapse margin ratio for 20% collapse probability

$ACMR_{10\%}$ = acceptable value of the adjusted collapse margin ratio for 10% collapse probability

The adjusted collapse margin ratio is the product of the collapse margin ratio, *CMR*, as determined from the response history analyses and a spectral shape factor, *SSF*, given in FEMA P695 (2009). The spectral shape factor depends on the fundamental period, *T*, and period based ductility, μ_T, and accounts for the frequency content of the selected ground motion record set.

$$ACMR_i = SSF_i\ CMR_i \tag{4}$$

The acceptable values of the adjusted collapse margin ratio are derived from the lognormal distribution and depend on the desired collapse probability (10% or 20%) and a measure of the total system collapse uncertainty (expressed as β_{total}). Uncertainty in the system collapse assessment comes from a number of sources. Uncertainty due to the variability between ground motions records is characterized by β_{RTR} [Equation 5 (FEMA 2009)]

$$\beta_{RTR} = 0.1 + 0.1\mu_T \leq 0.4 \tag{5}$$

Uncertainty in the design requirements, test data, and nonlinear modeling are characterized by qualitative quality ratings as will be described.

For both of systems, the design requirements have been well-vetted and provide extensive safeguards against unanticipated failure modes. The hierarchy of yielding and failure of components is well established. However, construction practices are comparatively less mature than for either structural steel or reinforced concrete structures. For these reasons, a quality rating of good (B) is given to the design requirements for both C-SMFs and C-SCBFs.

Numerous tests on composite members, connections, and frames have been conducted and reported in the literature. The tests span most of the important parameters which affect design requirements and the behavior is generally well understood. For these reasons, a quality rating of good (B) is given to the test data for both C-SMFs and C-SCBFs.

The nonlinear models directly simulate all predominate inelastic effects and have been extensively validated against experimental results. The sets of archetype frames provide a reasonably broad representation of the design space. However, fracture is not included in the modeling and the frames were assumed to be properly designed to preclude connection deterioration and lateral torsional buckling. For these reasons, a quality rating of good (B) is given to the nonlinear modeling for both C-SMFs and C-SCBFs.

The quality ratings are assigned lognormal standard deviation parameters [Table 6, (FEMA 2009)] and the total system collapse uncertainty is computed with Equation 6 then rounded to the nearest 0.025. The value depends on the period based ductility but is constant for $\mu_T \geq 3$. For both systems the value of β_{total} for $\mu_T \geq 3$ is 0.525.

$$\beta_{total} = \sqrt{\beta_{RTR}^2 + \beta_{DR}^2 + \beta_{TD}^2 + \beta_{MDL}^2} \tag{6}$$

Table 6. Quality Ratings

System	Quality of Design Requirements	Quality of Test Data	Quality of Nonlinear Modeling
C-SMF	B (Good) $\beta_{DR} = 0.2$	B (Good) $\beta_{TD} = 0.2$	B (Good) $\beta_{MDL} = 0.2$
C-SCBF	B (Good) $\beta_{DR} = 0.2$	B (Good) $\beta_{TD} = 0.2$	B (Good) $\beta_{MDL} = 0.2$

For the C-SMFs, all of the evaluations pass and thus the current response modification factor is deemed acceptable. In fact, all frames pass by a significant margin. Many of the IDA curves retain a significant positive slope even at the high levels of earthquake ground motion used in this study (up to 5-7 times maximum considered earthquake intensity). This is indicative of the excellent performance of C-SMFs subjected to earthquake ground motions. For the C-SCBFs, all of the evaluations pass and thus the current response modification factor is deemed acceptable. The margin of passing is not as great as for the C-SMFs, nonetheless, the C-SCBFs exhibit excellent performance. It should be noted that these results are only strictly applicable to well designed and detailed frames where connection deterioration will not occur and sufficient lateral bracing is provided.

7.3 Deflection Amplification Factor, C_d

According to the methodology, for systems with typical levels of damping, including the systems studied here, the deflection amplification factor, C_d, is equal to the response modification factor (FEMA 2009). For C-SCBFs this represents a minor change as the current difference between R and C_d is small and there structures are typically not displacement controlled. For C-SMFs this represents a significant change. Setting $C_d = R$ results in a 45% increase in C_d from the current value. Additionally, C_d plays a central role in the design of moment frames since they are often displacement controlled.

In this study, four frames were designed with the current C_d value. These frames had smaller members than their counterparts designed with $C_d = R = 8.0$. Some differences in performance were noted. The average overstrength of the frames designed with the current C_d was 4.9 while it was 6.4 for their counterparts. The average adjusted collapse margin ratio of the frames designed with the current C_d was 5.5 while it was 6.2 for their counterparts. These results indicate that the frames designed with the current C_d value have acceptable performance and that setting $C_d = R$ for this system is unnecessary from a safety perspective.

All in all, further study is needed to determine the ramifications of setting $C_d = R$ and whether such a change is necessary. Further study should include the possibility of a corresponding increase in the deformation limits should the C_d factor increase,

8. CONCLUSIONS

A study was conducted following recommendations in FEMA P695 (2009) to determine the seismic performance factors (i.e., R, C_d, and Ω_o) for composite special moment frames (C-SMF) and composite special concentrically braced frames (C-SCBF). A suite of 60 archetype frames was selected and designed according to current design specifications. Nonlinear static pushover analyses and dynamic response history analyses were performed on the frames to characterize the behavior and generate statistical data to be used in evaluation of the seismic performance factors. Both systems exhibited excellent seismic behavior and current seismic performance factors were found to be acceptable. In particular, it was noted that frames designed with the current deflection amplification factor, C_d, were found to be acceptable and thus a potential change to set $C_d = R$ should be studied further and perhaps accompanied by a corresponding change to the drift limits such that future seismic drift requirements are equivalent to the current seismic drift requirements.

Acknowledgements:

This material is based upon work supported by the National Science Foundation under Grant Nos. CMMI-0619047 and CMMI-0530756 as part of the George E. Brown, Jr. Network for Earthquake Engineering Simulation (NEES); the American Institute of Steel Construction; the Georgia Institute of Technology; and the University of Illinois at Urbana-Champaign. Computational analyses in this work were executed in part on the Extreme Science and Engineering Discovery Environment (XSEDE), which is supported by National Science Foundation Grant No. OCI-1053575. Any opinions, findings, and conclusions expressed in this material are those of the authors and do not necessarily reflect the views of the National Science Foundation or other sponsors.

References:

ACI. (2011). *Building Code Requirements for Structural Concrete and Commentary*. American Concrete Institute, Farmington Hills, MI.

AISC. (2010). *Seismic Provisions for Structural Steel Buildings*. American Institute of Steel Construction, Chicago, Illinois.

ASCE. (2010). *Minimum Design Loads for Buildings and Other Structures*. American Society of Civil Engineers, Reston, Virginia.

Bažant, Z. P., and Verdure, M. (2007). "Mechanics of Progressive Collapse: Learning from World Trade Center and Building Demolitions." *Journal of Engineering Mechanics*, 133(3), 308–319.

Denavit, M. D. (2012). "Characterization of Behavior of Steel-Concrete Composite Members and Frames with Applications for Design." Ph.D. Dissertation, University of Illinois at Urbana-Champaign, Urbana, Illinois.

FEMA. (2009). *Quantification of Building Seismic Performance Factors*. FEMA P695, Federal Emergency Management Agency, Washington, D.C.

Hsiao, P.-C., Lehman, D. E., and Roeder, C. W. (2012). "Improved Analytical Model for Special Concentrically Braced Frames." *Journal of Constructional Steel Research*, 73, 80–94.

Khandelwal, K., El-Tawil, S., and Sadek, F. (2009). "Progressive Collapse Analysis of Seismically Designed Steel Braced Frames." *Journal of Constructional Steel Research*, 65(3), 699–708.

Krawinkler, H., Medina, R., and Alavi, B. (2003). "Seismic Drift and Ductility Demands and their Dependence on Ground Motions." *Engineering Structures*, 25(5), 637–653.

Krishnan, S., and Muto, M. (2012). "Mechanism of Collapse of Tall Steel Moment Frame Buildings under Earthquake Excitation." *Journal of Structural Engineering*, ASCE, 138(11), 1361–1387.

McAllister, T., MacNeill, R., Erbay, O., Sarawit, A., Zarghamee, M., Kirkpatrick, S., and Gross, J. (2012). "Analysis of Structural Response of WTC 7 to Fire and Sequential Failures Leading to Collapse." *Journal of Structural Engineering*, ASCE, 138(1), 109–117.

NIST. (2010). *Evaluation of the FEMA P-695 Methodology for Quantification of Building Seismic Performance Factors*. National Institute of Standards and Technology, Gaithersburg, Maryland.

Szyniszewski, S., and Krauthammer, T. (2012). "Energy Flow in Progressive Collapse of Steel Framed Buildings." *Engineering Structures*, 42, 142–153.

Vamvatsikos, D., and Cornell, C. A. (2002). "Incremental Dynamic Analysis." *Earthquake Engineering & Structural Dynamics*, 31(3), 491–514.